LETTER

doi:10.1038/nature14017

The contribution of the Precambrian continental lithosphere to global H_2 production

Barbara Sherwood Lollar[1], T. C. Onstott[2], G. Lacrampe-Couloume[1] & C. J. Ballentine[3]

Microbial ecosystems can be sustained by hydrogen gas (H_2)-producing water–rock interactions in the Earth's subsurface and at deep ocean vents[1–4]. Current estimates of global H_2 production from the marine lithosphere by water–rock reactions (hydration) are in the range of 10^{11} moles per year[5–9]. Recent explorations of saline fracture waters in the Precambrian continental subsurface have identified environments as rich in H_2 as hydrothermal vents and seafloor-spreading centres[1,2] and have suggested a link between dissolved H_2 and the radiolytic dissociation of water[10,11]. However, extrapolation of a regional H_2 flux based on the deep gold mines of the Witwatersrand basin in South Africa[11] yields a contribution of the Precambrian lithosphere to global H_2 production that was thought to be negligible (0.009×10^{11} moles per year)[6]. Here we present a global compilation of published and new H_2 concentration data obtained from Precambrian rocks and find that the H_2 production potential of the Precambrian continental lithosphere has been underestimated. We suggest that this can be explained by a lack of consideration of additional H_2-producing reactions, such as serpentinization, and the absence of appropriate scaling of H_2 measurements from these environments to account for the fact that Precambrian crust represents over 70 per cent of global continental crust surface area[12]. If H_2 production via both radiolysis and hydration reactions is taken into account, our estimate of H_2 production rates from the Precambrian continental lithosphere of $0.36–2.27 \times 10^{11}$ moles per year is comparable to estimates from marine systems.

Ancient saline fracture waters in the Precambrian continental subsurface, with groundwater residence times ranging from millions[13] to billions of years[14], provide a previously underestimated source of H_2 for the terrestrial deep biosphere. Until now, little of the information on H_2 in these settings, accessed via underground research laboratories and mines, has been incorporated into global geochemical and biogeochemical models. Figure 1a documents (to our knowledge) the continental sites worldwide for which detailed H_2 studies have been published, as well as new data from our own research sites on the Precambrian Shield in Canada and South Africa (Table 1 and the source data for Fig. 1). Figure 1a shows that the high levels of H_2 reported for the Witwatersrand basin in South Africa by Lin *et al.*[1] are by no means a unique phenomenon. Sites in Precambrian terrains globally have H_2 concentrations as high as those reported for the Witwatersrand basin and for marine hydrothermal systems (Fig. 1a). Notably, sites on the Canadian and Fennoscandian Precambrian Shields and at Phanerozoic ophiolite seeps (such as in Luzon, Semail and Sonoma) and gas wells intersecting kimberlites (in Kansas), have even higher H_2 levels (>30% by volume) than those reported for the Witwatersrand basin (Table 1, Fig. 1a). The notable exposures of ultramafic and mafic rock at many of these sites are consistent with hydration of mafic/ultramafic rocks providing an additional source of H_2 at these sites above and beyond the H_2 produced by radiolysis. Drawing on this global data set, we provide, for the first time, estimates of global H_2 production for the Precambrian continental lithosphere that consider H_2 production from both radiolysis and hydration reactions.

When estimating radiolytic H_2 production, the ratio of H_2 to He (Fig. 1b) can provide important constraints, because He is an inert and conservative tracer. Using measured U, Th and K concentrations, natural α, β and γ particle fluxes can be estimated. Assuming a water-filled porosity of 0.1% and bulk rock density of 2.5 g cm^{-3}, Lin *et al.*[10] calculated radiolytic H_2 production rates in water ranging from 10^{-8} to 10^{-9} nM s^{-1} for granite, basalt and quartzite lithologies. The radiogenic ^{4}He production can also be estimated from U and Th abundances, allowing the H_2/He for radiolytic production of H_2 to be modelled (details in Methods). Since both radiogenic ^{4}He and radiolytic H_2 are correlated with U, Th and K concentrations, the H_2/He ratio is, for any given porosity, relatively insensitive to mineralogical composition (felsic, mafic or ultramafic), but is sensitive to porosity changes.

Here we use the Precambrian shield surface area of 1.06×10^8 km^2 (versus 1.48×10^8 km^2 for the total continental surface area) to scale the middle and upper continental crust ^{4}He production rate[15] to provide an estimate of the ^{4}He production rate for the Precambrian crust. Using H_2/He ratios as a function of porosity, we estimate H_2 production from radiolysis for the Precambrian continental lithosphere (details of all calculations in Methods). Estimates of porosity[16] vary from 1.6%–2% in the near surface, down to 0.2% at 10 km and 0.03% at 20 km, averaging 0.96% between 0 km and 10 km (upper crust) and 0.12% between 10 km and 20 km (middle crust). Calculated H_2/He values from radiolysis using the same assumptions as Lin *et al.*[11] yield average H_2/He values for the upper and middle continental crust of 117 and 15 for average porosities of 0.96% and 0.12%, respectively. Multiplying the ^{4}He production rate by the modelled H_2/He ratios yields a total radiolytic H_2 production rate in the water-filled fractures of the Precambrian crust of 0.16×10^{11} mol yr^{-1} (Table 2). This is a minimum estimate as it does not include basement rock fluid inclusions that also provide for at least an additional 1% water-filled porosity (see, for example, ref. 17). The latter would produce a further 0.31×10^{11} mol yr^{-1} to give a total Precambrian crustal H_2 production rate of at least 0.47×10^{11} mol yr^{-1} (Table 2). This is probably conservative given that if we used typical porosity values published for crystalline rock (up to 2%; details in Methods) rather than 0.12% to 0.96%, this value could be as high as $\sim 1 \times 10^{11}$ mol yr^{-1}. However, the key point is that even before considering H_2 production via hydration reactions, our estimate of H_2 from the Precambrian continental rocks based on radiolysis alone is similar to marine estimates (Table 2).

Since the discovery of H_2- and CH_4-rich fluids at the Lost City hydrothermal vents in the mid-Atlantic Ocean[18,19], there has been increasing interest in the role of water–rock reactions producing energy for chemosynthetic microbial communities, both in marine systems proposed to be analogues of the development of early biosynthetic pathways[20], and in continental Phanerozoic ophiolites[4,21]. Table 2 provides the estimates for high-temperature venting at the mid-ocean ridges[6,7], hydration reactions at vents and slow-spreading ridges[6,8,9,22], and Fe and sulphide oxidation of basaltic crust[5]—each of which are of the order of 10^{11} mol yr^{-1}. Although most of these studies refer to their estimates as H_2 flux, it would be more accurate to consider these to be H_2 production rates, as in fact only one of these[8] is strictly based on a diffusion flux model. The

[1]Department of Earth Sciences, 22 Russell Street, University of Toronto, Toronto M5S 3B1, Canada. [2]Department of Geosciences, Guyot Hall, Princeton University, Princeton, New Jersey 08544, USA. [3]Department of Earth Sciences, South Parks Road, University of Oxford, Oxford OX1 3AN, UK.

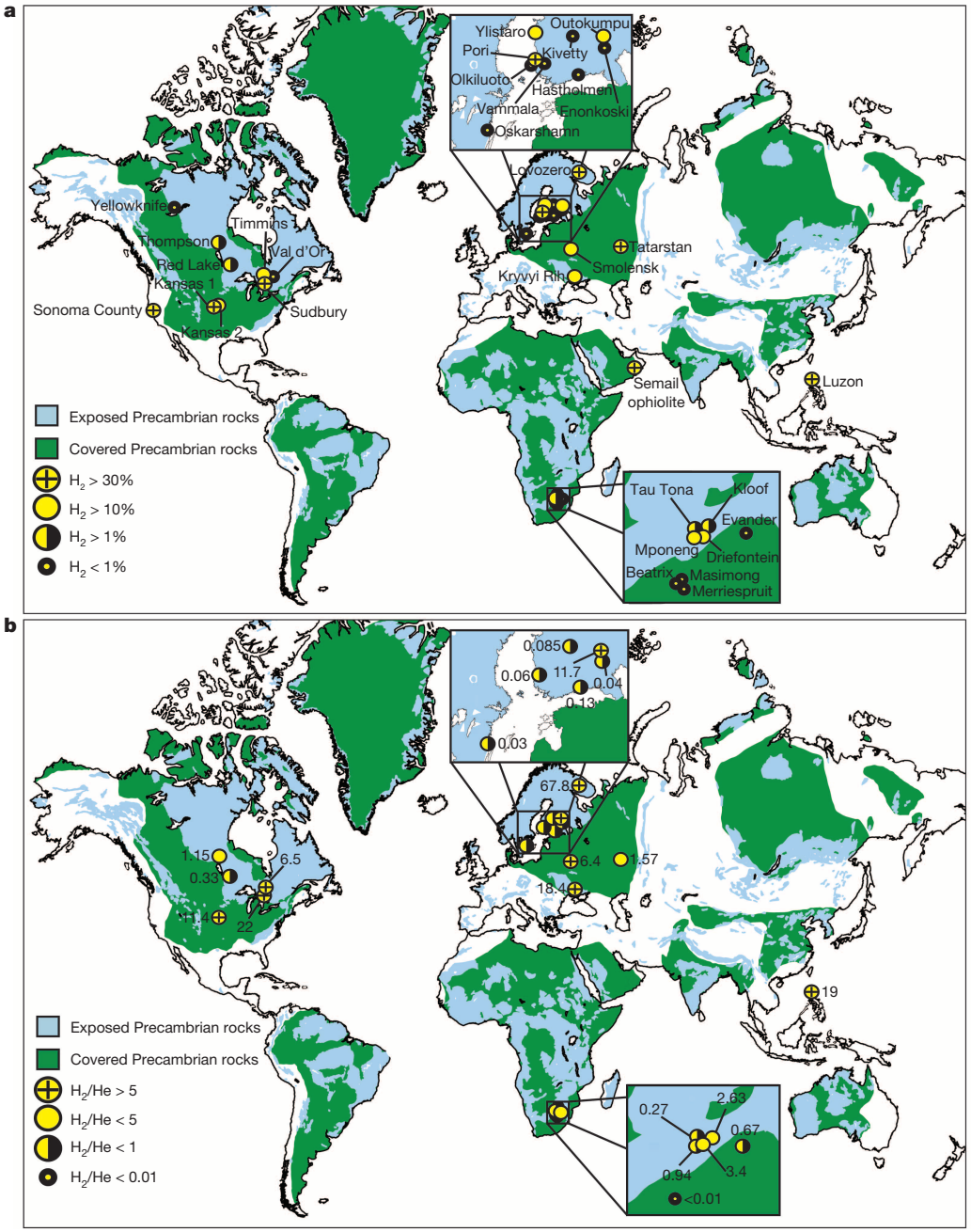

Figure 1 | Precambrian rocks of the continental crust. Geologic data are from ref. 12. Total Precambrian crust, exposed (blue) and buried (green), accounts for 1.06×10^8 km^2, or >70% of total continental crust surface area[12]. Symbols for each site show the highest reported H_2 levels in volume per cent (**a**) and H_2/He ratios (**b**), with locations provided in Table 1. H_2 concentrations and H_2/He ratios listed are the maximum observed at each location, but represent a minimum estimate owing to simultaneous H_2 consumption both by microbial communities of sulphate-reducers and methanogens[1] and reaction of H_2 to produce abiogenic hydrocarbons via Fischer–Tropsch synthesis[21,28]. Map generated via open source software from ref. 29.

others follow the approach typical for this literature, using reaction-based models with a governing equation relating oxidation of FeO in the crust to H_2 production such as the following from Sleep and Bird[6]:

$$3\text{FeO (in silicates)} + H_2O \rightarrow Fe_3O_4 \text{ (magnetite)} + H_{2(aq)} \quad (1)$$

Depending on the study, FeO contents are assumed to be between 5% and 10%, reaction efficiencies range from 100% to the more conservative estimate[6] of 50%, and typical rock densities fall in the range 3,000–3,500 kg m^{-3}. These estimates from the marine lithosphere yield H_2 production estimates in moles per square metre of surface area for oceanic crust to an assumed depth of 1 km. These reaction model calculations are then coupled to estimates of hydrothermal fluid or water circulation through the spreading centres or ocean floor[7] or to ocean crust production rates[5,6] to introduce a temporal term and finally express H_2 production in terms of moles per year (Table 2 and Methods).

To provide the most relevant comparison to the marine literature, we took a similar reaction model approach (detailed calculations in Methods). The iconic greenstone belts of the Precambrian, named for the coloration of the mafic/ultramafic minerals, formed initially as island arcs, continental margin arcs, submarine plateaus, oceanic islands and in some cases, Archean oceanic crust[23]. Owing to fundamental changes in the nature of volcanism and heat flux[24], the greatest production (and thickness) of greenstone terrains are in the Archean, although formation continued

Table 1 | Maximum H_2 and H_2/He at Precambrian sites and selected Proterozoic ophiolites

Site Name	Location	Latitude	Longitude	H_2	H_2/He
Red Lake	Canada	51° 4′ 20.9″ N	93° 46′ 45.9″ W	1.60%	0.33
Sudbury	Canada	46° 29′ 33.8″ N	81° 0′ 38.4″ W	57.8%	22
Thompson	Canada	55° 44′ 51.0″ N	97° 51′ 4.7″ W	2.75%	1.15
Timmins	Canada	48° 28′ 42.2″ N	81° 19′ 55.3″ W	12.7%	6.5
Val D'Or	Canada	48° 6′ 26.8″ N	77° 47′ 11.1″ W	0.51%	NA
Yellowknife	Canada	62° 27′ 46.2″ N	114° 22′ 41.1″ W	<0.01%	NA
Enonkoski	Finland	62° 5′ 22.0″ N	28° 54′ 57.9″ E	0.04%	0.04
Hastholmen	Finland	60° 1′ 44.0″ N	24° 9′ 23.0″ E	1.1%	0.13
Kivetty	Finland	62° 50′ 7.8″ N	25° 39′ 2.6″ E	0.001%	0.085
Olkiluoto	Finland	61° 14′ 19.0″ N	21° 28′ 33.0″ E	0.11%	0.06
Outokumpu	Finland	62° 43′ 34.1″ N	29° 0′ 58.7″ E	12.8%	11.7
Pori	Finland	61° 29′ 12.1″ N	21° 47′ 53.5″ E	30.4%	NA
Vammala	Finland	61° 20′ 28.5″ N	22° 54′ 34.8″ E	<0.01%	NA
Ylistaro	Finland	62° 56′ 25.8″ N	22° 30′ 47.1″ E	11.4%	NA
Beatrix	S. Africa	27° 58′ 28.9″ S	26° 44′ 4.2″ E	<0.01%	<0.01
Driefontein	S. Africa	26° 23′ 60.0″ S	27° 30′ 0.0″ E	10.3%	3.4
Evander	S. Africa	26° 24′ 59.0″ S	29° 4′ 59.5″ E	0.01%	0.67
Kloof	S. Africa	26° 20′ 51.3″ S	27° 37′ 27.1″ E	9.25%	2.63
Masimong	S. Africa	27° 55′ 60.0″ S	26° 45′ 0.0″ E	<0.01%	NA
Merriespruit	S. Africa	28° 6′ 60.0″ S	26° 51′ 0.0″ E	<0.01%	NA
Mponeng	S. Africa	26° 25′ 30.0″ S	27° 24′ 60.0″ E	11.5%	0.94
TauTona	S. Africa	26° 23′ 60.0″ S	27° 24′ 60.0″ E	2.40%	0.27
Oskarshamn	Sweden	57° 24′ 51″ N	16° 39′ 55″ E	0.08%	0.03
Lovozero	Russia	67° 51′ 2.5″ N	35° 5′ 58.2″ E	35.2%	67.8
Tatarstan	Russia	55° 12′ 59.4″ N	50° 45′ 11.4″ E	96.1%	1.57
Smolensk	Russia	54° 47′ 6.9″ N	32° 3′ 1.6″ E	13.5%	6.49
Kryvyi Rih	Ukraine	47° 55′ 0.0″ N	33° 15′ 0.0″ E	23.2%	18.4
Kansas 1	USA	38° 48′ 19.7″ N	96° 52′ 5.8″ W	80.0%	NA
Kansas 2	USA	39° 56′ 17.4″ N	95° 30′ 20.7″ W	17.2%	11.4
Sonoma	USA	39° 5′ 45.5″ N	122° 26′ 20.3″ W	51.7%	NA
Semail	Oman	20° 36′ 44.0″ N	55° 58′ 57.6″ E	99.0%	NA
Luzon	Philippines	16° 38′ 48.2″ N	121° 15′ 54.9″ E	42.6%	19

The table shows the maximum reported H_2 concentrations (in volume per cent of total gas phase) and maximum observed H_2/He ratios (see text) for each site in the Precambrian subsurface shown in Fig. 1, with values for boreholes intersecting kimberlites from Kansas, USA; and samples from younger, surface-exposed Phanerozoic ophiolites (Sonoma County, California; Semail, Oman; and Luzon, Philippines) shown for comparison. In addition to >50 new boreholes/samples published here for the first time, ~150 other boreholes/samples have been compiled from the literature in order to provide a quantitative global context for this phenomenon. For individual data points see the source data for Fig. 1 and for site locations and geologic descriptions see Methods. NA, not analysed.

more rarely throughout the later geologic record[23]. Precambrian greenstone sequences can be many kilometres thick[23,25] and thus differ fundamentally from the Phanerozoic continental ophiolites (relatively thin splinters of oceanic crust obducted onto the continents) that have been the focus of most H_2 production studies so far. Of the total surface area of the continents (1.48×10^8 km^2; ref. 12), exposed Precambrian crust, including the uplifted exposed cratons (shown as the blue-shaded areas in Fig. 1), accounts for approximately 30% of the total continental surface area. Including both exposed cratons (blue) and Precambrian crust beneath consolidated Phanerozoic sediments (green-shaded areas in Fig. 1) the total Precambrian crust accounts for 72% of the continents (or 1.06×10^8 km^2; ref. 12). Using this value for the total Precambrian continental crust, and based on estimates from ref. 12 that 86% is Proterozoic (9.12×10^7 km^2) and 14% is Archean (1.48×10^7 km^2), and using the 25% and 50% of mafic/ultramafic rock abundance for Proterozoic and Archean crust respectively[26], using a depth of 1 km, we obtain a combined Precambrian rock volume with H_2 production potential via hydration reactions of 3.02×10^{16} m^3 (Extended Data Table 1).

Table 2 | Estimates of H_2 production from water–rock reactions

System	H_2 production (10^{11} mol yr^{-1})	Reference
Ocean crust	0.8 to 1.3	Ref. 7
Ocean crust	1.9	Ref. 6
Ocean crust	2.0	Ref. 9
Slow-spreading ridges	1.67	Ref. 8
Basaltic ocean crust	4.5 ± 3.0	Ref. 5
Continental Precambrian radiolysis	0.16 to 0.47	This study
Continental Precambrian hydration reactions	0.2 to 1.8	This study

The table shows global estimates of H_2 production from water–rock alteration reactions (in units of 10^{11} mol yr^{-1}) from marine lithosphere and H_2 production estimates from radiolysis and hydration of mafic/ultramafic rocks from Precambrian continental lithosphere derived in this study. Estimates made using conservative assumptions. For details of all calculations see Methods. Volcanic, mantle-derived or microbial sources of H_2 are not incorporated.

Although the total thickness of the continental crust is between 30 km and 50 km, we based our estimate on a depth of 5 km, the estimated depth of the habitable zone[6] (details in Methods). Assuming a rock density of 3,000 kg m^{-3}, an average FeO of 10% for these mafic/ultramafic rocks (based on the values of 9.2% to 11.3% given by ref. 27), and a FeO:H_2 ratio of 3:1 as in equation (1), and incorporating the age of the rock, we obtain an estimate of $0.78–1.8 \times 10^{11}$ mol yr^{-1} H_2 from the mafic/ultramafic Precambrian crust (Extended Data Table 2).

A more conservative lower boundary can be calculated by incorporating the variation in reaction efficiency. Rather than using 100% reaction efficiency ($\Delta\xi = 1$), as above, we used a second approach that assumes $\Delta\xi = 1/2$ in the uppermost kilometre, $\Delta\xi = 1/4$ in the second kilometre, $\Delta\xi = 1/8$ in the third kilometre, and so on as in ref. 6. Applying this series to the H_2 production rate of $0.78–1.8 \times 10^{11}$ mol yr^{-1} produces a minimum estimate of $0.2–0.4 \times 10^{11}$ mol yr^{-1} (details in Methods). These upper (1.8×10^{11}) and lower (0.2×10^{11}) boundary estimates are provided in Table 2. Even these are probably conservative, because alternative methods of calculating production rate—based on incorporation of exhumation rates or on extrapolation of published experimental rates of H_2 generation via hydration reactions—all yield estimates of H_2 production that are even higher (details in Methods).

These findings all support the major conclusion of this paper that H_2 production from the Precambrian continental lithosphere, hitherto assumed to be negligible, is in fact an important source of H_2 production. Although H_2 estimates from marine systems provide an important end-member, we suggest that a thorough assessment of the global H_2 potential for supporting a deep subsurface biosphere should not neglect the Precambrian terrain. H_2 production from either radiolysis or hydration of mafic/ultramafic rocks alone revises upward previous published estimates of global H_2 production. The initial estimates provided here suggest that incorporation of H_2 production from the Precambrian continental lithosphere could double existing estimates of global H_2 production from these processes that have been based on marine systems alone.

Online Content Methods, along with any additional Extended Data display items and Source Data, are available in the online version of the paper; references unique to these sections appear only in the online paper.

Received 30 July; accepted 27 October 2014.

1. Lin, L.-H. *et al.* Long-term sustainability of a high-energy, low-diversity crustal biome. *Science* **314,** 479–482 (2006).
2. Sherwood Lollar, B. *et al.* Hydrogeologic controls on episodic H_2 release from Precambrian fractured rocks—energy for deep subsurface life on Earth and Mars. *Astrobiology* **7,** 971–986 (2007).
3. D'Hondt, S. *et al.* Subseafloor sedimentary life in the South Pacific gyre. *Proc. Natl Acad. Sci. USA* **106,** 11651–11656 (2009).
4. Schrenk, M. O., Brazelton, W. J. & Lang, S. Q. Serpentinization, carbon, and deep life. *Rev. Mineral. Geochem.* **75,** 575–606 (2013).
5. Bach, W. & Edwards, K. J. Iron and sulfide oxidation within the basaltic ocean crust: implications for chemolithoautotrophic microbial biomass production. *Geochim. Cosmochim. Acta* **67,** 3871–3887 (2003).
6. Sleep, N. H. & Bird, D. K. Niches of the pre-photosynthetic biosphere and geologic preservation of the Earth's earliest ecology. *Geobiology* **5,** 101–117 (2007).
7. Canfield, D. E., Rosing, M. T. & Bjerrum, C. Early anaerobic metabolisms. *Phil. Trans. R. Soc. Lond. B* **361,** 1819–1836 (2006).
8. Cannat, M., Fontaine, F. & Escartin, J. Serpentinization and associated hydrogen and methane fluxes at slow spreading ridges. *AGU Geophys. Monogr. Ser.* **188,** 241–264 (2010).
9. Kasting, J. F. & Canfield, D. E. in *Fundamentals of Geobiology* (eds Knoll, A. H., Canfield, D. E. & Konhauser, K. O.) Ch. 7, 93–104 (Blackwell, 2012).
10. Lin, L.-H., Slater, G. F., Sherwood Lollar, B., Lacrampe-Couloume, G. & Onstott, T. C. The yield and isotopic composition of radiolytic H_2, a potential energy source for the deep subsurface biosphere. *Geochim. Cosmochim. Acta* **69,** 893–903 (2005a).
11. Lin, L.-H. *et al.* Radiolytic H_2 in the continental crust: nuclear power for deep subsurface microbial communities. *Geochem. Geophys. Geosyst.* **6,** Q07003 (2005b).
12. Goodwin, A. M. *Principles of Precambrian Geology* (Academic, 1996).
13. Lippmann-Pipke, J. *et al.* Neon identifies two billion year old fluid component in Kaapvaal Craton. *Chem. Geol.* **283,** 287–296 (2011).
14. Holland, G. *et al.* Deep fracture fluids isolated in the crust since the Precambrian. *Nature* **497,** 357–360 (2013).
15. Ballentine, C. J. & Burnard, P. G. Production, release and transport of noble gases in the continental crust. *Rev. Mineral. Geochem.* **47,** 481–538 (2002).
16. Bethke, C. M. A numerical model of compaction-driven groundwater flow and heat transfer and its appplication to the paleohydrology of intracratonic sedimentary basins. *J. Geophys. Res.* **90,** 6817–6828 (1985).
17. Nordstrom, D. K., Lindblom, S., Donahoe, R. J. & Barton, C. C. Fluid inclusions in the Stripa granite and their possible influence on the groundwater chemistry. *Geochim. Cosmochim. Acta* **53,** 1741–1755 (1989).
18. Kelley, D. S. *et al.* A serpentinite-hosted ecosystem: the Lost City Hydrothermal Field. *Science* **307,** 1428–1434 (2005).
19. Proskurowski, G. *et al.* Abiogenic hydrocarbon production at Lost City Hydrothermal Field. *Science* **319,** 604–607 (2008).
20. Lang, S. Q. *et al.* Microbial utilization of abiogenic carbon and hydrogen in a serpentinite-hosted system. *Geochim. Cosmochim. Acta* **92,** 82–99 (2012).
21. Etiope, G. & Sherwood Lollar, B. Abiotic methane on Earth. *Rev. Geophys.* **51,** 276–299 (2013).
22. Sleep, N. H., Meibom, A., Fridriksson, T., Coleman, R. G. & Bird, D. K. H_2-rich fluids from serpentinization: geochemical and biotic implications. *Proc. Natl Acad. Sci. USA* **101,** 12818–12823 (2004).
23. Condie, K. C. Greenstones through time. In *Archean Crustal Evolution* (ed. Condie, K. C.) Ch. 3, 85–120 (Elsevier, 1994).
24. Bickle, M. J. Implications for melting for stabilization of the lithosphere and heat loss in the Archean. *Earth Planet. Sci. Lett.* **80,** 314–324 (1986).
25. de Wit, M. & Ashwal, L. D. *Greenstone Belts* (Oxford Monographs on Geology and Geophysics Vol. 35, Clarendon Press, 1997).
26. Condie, K. C. Chemical composition and evolution of the upper continental crust: contrasting results from surface samples and shales. *Chem. Geol.* **104,** 1–37 (1993).
27. Rudnick, R. L. & Fountain, D. M. Nature and composition of the continental crust: a lower crustal perspective. *Rev. Geophys.* **33,** 267–309 (1995).
28. Onstott, T. C. *et al.* Martian CH_4: sources, flux and detection. *Astrobiology* **6,** 377–395 (2006).
29. Chorlton, L. B. *Generalized Geology of the World: Bedrock Domains and Major Faults in GIS format: A Small-scale World Geology Map with an Extended Geological Attribute Database* Open File 5529 (Geological Survey of Canada, 2007).

Acknowledgements The preparation and execution of this work was supported by the Canada Research Chairs programme, NSERC Discovery and Accelerator grants to B.S.L. with additional partial funding from the Sloan Foundation Deep Carbon Observatory, Canadian Space Agency and National Science Foundation grant number EAR-0948659.f. We are grateful to K. Chu, A. Yang and G. S. Lollar (of the University of Toronto) for preparation of the maps and tables and to N. Sleep, H. D. Holland, J. Mungall and M. A. Hamilton for discussions on Precambrian geology and mineralogy. We also thank colleagues and supporters at the mines and underground research laboratories whose efforts resulted in the original primary publications from which a portion of this data set is compiled.

Author Contributions B.S.L. designed the project and wrote the paper. B.S.L., C.J.B. and T.C.O. developed the models for H_2 generation. All co-authors contributed to the interpretation and final version of the manuscript.

Author Information Reprints and permissions information is available at www.nature.com/reprints. The authors declare no competing financial interests. Readers are welcome to comment on the online version of the paper. Correspondence and requests for materials should be addressed to B.S.L. (bslollar@chem.utoronto.ca).

METHODS

In Table 1, for each site, the maximum measured H_2 (percentage of total gas) and H_2/He are reported. Maximum H_2/He ratios provide a conservative (minimum) measure of H_2 production, given that there has probably been loss of H_2 to biological and chemical sinks relative to inert He[1,11,21,22,28], as has also been noted by studies for the marine H_2 sub-seafloor biosphere where measured H_2 concentrations were low or below detection limit for many samples[3,30]. Specific measurements of H_2 and H_2/He for each of the >200 samples/boreholes, including 56 previously unpublished, are provided in the source data for Fig. 1. Data are for gases discharging from exploration boreholes in subsurface mines at 19 Precambrian Shield sites from Canada, Finland and South Africa[2,31–34]. Originally dissolved in saline groundwater in sealed fracture systems in the rocks, gases are released via depressurization into mine workings at rates of 1 to >30 litres of gas per minute per borehole[14,34]. For comparison, samples from 13 additional sites are included[35–43] for a total of 32 sites worldwide (see source data for Fig. 1). Although marine and groundwater systems can typically report all measurements as dissolved moles per litre, the database in this paper is drawn from degassing boreholes, in some cases from gas seeps with no corresponding water flow, or from historic data, as well as from fluid inclusions results. The data are all therefore reported as volume per cent of the total gas phase as the only commonly available unit. Sampling methods are described in the relevant publications for each site, and for the mine boreholes in Canada, Finland and South Africa in refs 14 and 33. Compositional analyses of gas samples were performed after the methods of ref. 33. All analysis were run in triplicate and mean values are reported. Reproducibility for triplicate analyses is ±5%. Additional details of the geologic settings, sampling methods and analytical methods are provided in the specific references for each site (listed above and in the source data for Fig. 1).

Previous radiolytic H_2 estimates for Precambrian continents. Natural emission of α, β and γ particles released due to decay of U, Th and K was calculated by Lin *et al.*[10] for representative granite, basalt and quartzite lithologies as the basis for calculating radiolytic H_2 production. For each lithology a water-filled porosity of 0.1% and bulk rock density of 2.5 g cm^{-3} was used and stopping powers of 1.5, 1.25 and 1.14 were used for α, β and γ particles respectively. Lin *et al.*[10] calculated the rate of H_2 accumulation within the water from radiolysis (that is, the H_2 production rate in water) to be 9.0×10^{-8}, 9.4×10^{-9} and 2.6×10^{-8} nM s^{-1}, respectively, on the basis of typical ranges of U, Th and K contents for granite, basalt and quartzite lithologies. H_2 production rates of approximately 10^{-8} nM s^{-1} were reported for a range of felsic lithologies, while for a range of U, Th and K contents typical of mafic and ultramafic lithologies[26,44] values of 10^{-9} nM s^{-1} were calculated[10].

Lin *et al.*[11] used a steady-state diffusive flux model to calculate a regional flux of H_2 from radiolysis out of the topmost 20 km of the Witwatersrand basin. Using the estimates of ^{4}He production and H_2 production for the different stratigraphic formations of the Witwatersrand basin, as described above, assuming a water-filled effective porosity of 1% and complete interconnection of pore space, they used a steady-state diffusion model, the diffusion coefficient for H_2 in water[45], and a dC/dz term based on calculating concentration gradients between the stratigraphic formation thickness of the Witwatersrand basin units, to derive a concentration C versus depth z profile for dissolved H_2 in the water. From this they estimated a regional flux specific to the Witwatersrand basin of ~8 μmol m^{-2} yr^{-1} of H_2 produced by radiolysis[10,11]. Given the surface area of the Witwatersrand basin of 5.25×10^{10} m^2 (~350 km × 150 km), this corresponds to a H_2 diffusive flux of 4.2×10^5 mol yr^{-1}, which, if extrapolated to the surface area of the Precambrian continents (1.06×10^8 km^2) yields a global H_2 flux estimate of 0.009×10^{11} mol yr^{-1}. Based on these estimates, and on the prevailing assumption that radiolysis is the sole H_2-generating mechanism, the contribution of the Precambrian continental lithosphere to global H_2 production has typically been neglected (for example, in ref. 6), since global estimates from alteration of oceanic crust are typically two orders of magnitude higher (Table 2).

It is unlikely that the Witwatersrand basin can be considered truly steady state in terms of diffusion. The diffusion models on which the Lin *et al.*[11] model was based were developed for sedimentary basins rather than crystalline fractured rock. An inherent limitation is using a regional estimate such as this (dependent on the specific formation thicknesses and H_2 concentrations of one regional basin) to extrapolate to a global estimate. Most importantly, by focusing only on H_2 dissolved in fracture waters (H_2 production in waters), this estimate neglects any ^{4}He and H_2 stored in the lithological formations. Lin *et al.*[11] assumed that all of the ^{4}He was released from the mineral phases to the pore water, after the method of ref. 46. It is necessarily therefore an underestimate of overall radiolytic H_2 production in these rocks. Here we attempt to address this by focusing instead on developing an estimate based on lithology production rates for H_2 (production rate within a given volume of lithology).

Radiolytic H_2 estimates for Precambrian continents. In this study, we discuss how the ratio of ^{4}He to radiolytic H_2 production changes as a function of depth in the crust, and we use the continental ^{4}He production rate and calculated ^{4}He/H_2 ratios to estimate radiolytic H_2 production from the continental crust. The contributions of H_2 to both the water-filled fracture porosity, and to storage in the form of fluid inclusions, are included in this approach (see main text). The production of ^{4}He and radiolytic production of H_2 in the continental crust are due to the radioelements U and Th (and K, which produces H_2 but does not produce ^{4}He). For a given porosity, H_2 and ^{4}He production rates scale to the radioelement concentrations of the host rock. Hence production rates for H_2 and ^{4}He are correlated, and H_2/He ratio and H_2 lithology production rates increase with increasing porosity.

Reported porosities for granite basement rocks range between 0.9% and 2.3% (ref. 47). Bucher and Stober[48] report a characteristic porosity for basement rocks of 1.0%, while well tests for effective porosities for the Black Forest basement[49] and from the Canadian Shield[50] report a range from 0.1% to 2.1%. To incorporate changes in porosity with depth in the crust, the minimum water available for radiolysis in the continental crust can be estimated by assuming a water-filled fracture porosity T that exponentially declines with depth in kilometres z after the models of ref. 16:

$$T = 1.6e^{-z/4.8} \quad (2)$$

This porosity expression yields a porosity that varies from 1.6% down to 0.2% at 10 km and 0.03% at 20 km, averaging 0.96% between 0 km and 10 km (upper crust) and 0.12% between 10 km and 20 km (middle crust)[16]. The porosities predicted by this expression are compatible with He porosities measured in rock units from the Witwatersrand basin[51] and fracture porosities in other crystalline systems[47–50]. Calculated H_2/He values from radiolysis using the same assumptions as Lin *et al.*[11] then yield average H_2/He values for the upper and middle continental crust of 117 and 15 for average porosities of 0.96% and 0.12%, respectively.

The continental crust ^{4}He production rates based on the radioelement content of the upper and middle continental crust are estimated to be 1.8×10^8 mol yr^{-1} and 1.6×10^8 mol yr^{-1} (ref. 15). The lower continental crust accounts for ~6% of the ^{4}He (ref. 15) and we neglect this portion of the crust in these calculations. Given that ~70% of the remaining continental crust is comprised of Precambrian basement[12], the production of H_2 from the upper and middle Precambrian shield is 1.2×10^8 mol yr^{-1} and 1.1×10^8 mol yr^{-1}. Using the H_2/He values calculated above for the fracture porosity (117 and 15 respectively) yields H_2 production in the upper and middle crust of 1.44×10^{10} mol yr^{-1} and 1.64×10^9 mol yr^{-1} to give an initial Precambrian crust fracture porosity H_2 production rate of 0.16×10^{11} mol yr^{-1} (Table 2).

The fracture porosity estimate alone, however, is an underestimate of the H_2O volume exposed to irradiation, because it does not include the fluid inclusion volume, which for basement rocks is typically at least 1% (for example, ref. 17). Radiolytically produced H_2 has been reported in fluid inclusions[52] and their migration into the fracture water can occur via solid-state diffusion through the host mineral phase, or episodically through metamorphic/tectonic events[53] or inclusion decrepitation via fracture propagation[13]. We assumed that the decreasing density of water with increasing temperature and pressure was offset by increasing salinity so that the water density remained ~1 g cm^{-3}. Calculated H_2/He values from radiolysis in water-filled fluid inclusions following Lin *et al.*[11] yields minimum H_2/He values for the upper and middle continental crust of 133 and 135 in this case. As above, using the calculated H_2/He values for the water-filled fluid inclusions yields H_2 production in the upper and middle crust of 0.16×10^{11} mol yr^{-1} and 0.15×10^{11} mol yr^{-1} to give a total Precambrian crust fluid inclusion H_2 production rate of 0.31×10^{11} mol yr^{-1}. The sum of the fracture porosity (0.16×10^{11} mol yr^{-1}) and fluid inclusion estimates (0.31×10^{11} mol yr^{-1}) produces a calculated H_2 Precambrian crustal production rate of 0.47×10^{11} mol yr^{-1} (Table 2).

This is a conservative estimate, because the porosity-to-depth relationships used reflect average values of porosity. Using the function from ref. 16, which gives a value of 0.96% average porosity for the upper crust and 0.12% for the lower crust, means that in essence we have taken the average porosity of the crust to be (1.0 + 0.12)/2 = 0.56%. For the more representative estimates of porosity for crystalline rock of 1% to 2% described above, the estimated H_2 production from radiolysis could be as high as 1×10^{11} mol yr^{-1}. Importantly, even before an estimate is incorporated for H_2 production via hydration reactions, this estimate of H_2 from the Precambrian continental rocks based on radiolysis alone is similar to marine estimates (Table 2).

H_2 production from hydration reactions in marine systems. Several studies have produced estimates of global H_2 production from marine systems, including both volcanic/magmatic sources (not considered here) and H_2 production from the abiogenic water–rock alteration reactions that are the focus of this paper. Table 2 provides the estimates for high-temperature venting at the mid-ocean ridges[6,7], for warm vents and slow-spreading ridges[6,8,9,22], as well as for Fe and sulphide oxidation of basaltic crust[5]. Only one of these marine studies[8] is based on a diffusion model. All the others follow the approach typical for the marine literature, using reaction-based models with a governing equation relating oxidation of FeO in the crust to H_2 production at a ratio of between 3:1 to 2:1 that is either of the form of equation (1) of ref. 6, or of the following form, from refs 5 and 7:

$$3Fe_2SiO_4 + 2H_2O \rightarrow 3SiO_2 + 2Fe_3O_4 + 2H_{2(aq)} \quad (3)$$

All the marine studies cited in Table 2 use the following assumptions: FeO content typically between 5% and 10%; reaction efficiency $\Delta\xi$ varying from 100% ($\Delta\xi = 1$) to the more conservative estimate from ref. 6 of 50% ($\Delta\xi = 0.5$); and rock density of 3,000–3,500 kg m^{-3}. These marine literature estimates then calculate H_2 production in moles per square metre of surface area for oceanic crust to a depth of typically 1 km and are then coupled to estimates of hydrothermal fluid or water circulation through the spreading centres or ocean floor[7] or to ocean crust production rates[5,6] to introduce a temporal term and then express H_2 production in terms of moles per year (Table 2). Two of the cited studies take a slightly different approach, based on empirical measurements (see discussion below)[8,9].

Definition of terms for flux versus production estimates. As the details above indicate, the major references cited in the field for marine global H_2 flux estimates are actually based on reaction-based models rather than diffusion models in many cases. Each of the above papers calculated global H_2 flux from marine water–rock reaction models, as outlined above. In this sense, only ref. 8 can strictly be called a flux estimate, yet—importantly—all the cited papers used the term 'H_2 flux' to describe the results of their reaction-based models. Only ref. 5 use what is likely to be the more appropriate term: 'production rate'. To provide the best basis of comparison to the marine estimates, we took a similar reaction-based approach for the calculation of H_2 production in this study, as outlined in detail below. For consistency, we have also chosen to use 'production rate' to refer to both the previously published marine estimates and the continental Precambrian estimates resulting from this study (Table 2).

Definition of terms for H_2 production via hydration reactions. Although the term serpentinization specifically refers to reaction of the Mg-rich olivine end-member (Fo) to produce serpentine, brucite and magnetite, it is in fact widely used as an umbrella term encompassing a suite of reactions all of which produce H_2 as a by-product of hydration of mafic and ultramafic minerals[4,8,21,54]. Recent experimental work supports this, demonstrating that H_2 production can occur under a range of temperatures and minerals, including mafic and ultramafic rocks containing peridotite, pyroxene, olivine and magnetite[55,56]. It is in this sense that the term serpentinization is used here, encompassing the full range of hydration and redox reactions that produce H_2 from alteration of ultramafic and mafic rock.

H_2 production from hydration reactions in Precambrian rocks. In this study, we took a reaction model approach similar to those in the marine literature references described above, using equation (1) from ref. 6, assuming a rock density of 3,000 kg m^{-3}, and initially an extent of reaction of $\Delta\xi = 1$. It is important to note that the Precambrian continental crust differs substantially from average continental crust in certain pertinent parameters, in particular, the proportion of mafic and ultramafic rocks and hence FeO content. While the Phanerozoic continental crust is composed of <20% mafic/ultramafic rock, the percentage increases in the Precambrian and is estimated at 25% of Proterozoic crustal rock and between 45% and 51% of the Archean crust[26] (Extended Data Table 1). In addition, whereas the total continental crust has an average FeO weight per cent of only 6.6%, the more mafic and ultramafic Archean and Post-Archean rocks range between 9.2% and 11.3% (ref. 27).

Of the total surface area of the continents (1.48×10^8 km^2; ref. 12), exposed Precambrian crust (including the uplifted exposed cratons (for example, the Canadian Shield, Kola Peninsula, the Kaapval Craton) shown as the blue shaded areas in Fig. 1) accounts for approximately 30% of the total continental surface area. Including both exposed cratons (blue) and Precambrian crust beneath consolidated Phanerozoic sediments (green shaded areas in Fig. 1) accounts for 72% of the continental crust (or 1.06×10^8 km^2; ref. 12). Using this value for the total Precambrian continental crust, and based on estimates from ref. 12, 86% is Proterozoic in age (9.12×10^7 km^2) and 14% is Archean (1.48×10^7 km^2) (Extended Data Table 1). Knowing from ref. 26 that approximately 25% of the Proterozoic is ultramafic/mafic in composition; and approximately 50% of the Archean is ultramafic/mafic, then for a 1 km depth of crust the volume that has H_2 production potential can be estimated to be 2.28×10^{16} m^3 (Proterozoic) and 0.74×10^{16} m^3 (Archean) respectively.

Assuming a rock density of 3,000 kg m^{-3}, an average FeO of 10% for these mafic/ultramafic rocks (based on the values of 9.2% to 11.3% from ref. 27), and a FeO:H_2 ratio of 3:1 as per equation (1), then H_2 production from the ultramafic/mafic Precambrian can be calculated as follows:

$$(3 \times 10^6\ \mathrm{g\,m^{-3}} \times 0.1)/(3 \times 71.845)\ \mathrm{g\,mol^{-1}} = 1.4 \times 10^3\ \mathrm{moles\ H_2\,m^{-3}} \quad (4)$$

Over a depth of 1 km, this corresponds to an estimate of 3.19×10^{19} moles H_2 from the Proterozoic crust and 1.04×10^{19} moles H_2 from the Archean crust. Over an estimated habitable zone of 5 km depth[6], the above estimates scale to 16.0×10^{19} moles H_2 and 5.2×10^{19} moles H_2 respectively (Extended Data Table 1).

Incorporation of temporal component. Estimates of H_2 production from the marine crust typically convert such reaction-based estimates of H_2 production for a given volume of oceanic crust by incorporating time, either by coupling estimates of total moles H_2 produced to the estimated rate of formation of ocean crust, or by coupling estimates of the rate of hydrothermal fluid circulation and heat flux[5–7]. Fluid circulation within Precambrian cratons is more difficult to estimate. However, even in the absence of active tectonism in the Precambrian continents, stress-induced fracturing due to erosion and uplift, and penetration by fracture waters will continue to drive hydration reactions at some finite rate. Typical conceptual models for such systems envisage (1) fracture fluids driving local chemical gradients and renewal of reaction zones at the mineral and fracture interfaces[55]; (2) positive feedback mechanisms wherein reaction-driven cracking further increases permeability and reactive surface areas[57]; and (3) episodic H_2 production due to destabilization of mineral surfaces during progressive water–rock reactions[2,56]. The episodic nature of these fracture and fluid driven processes means that reaction times will necessarily then be smaller than the total age of the rock. In the absence of detailed information on reaction zones and rates in natural systems, however, by using the age of the rocks as a first approximation, we can derive a conservative estimate of rate. Actual rates could only be larger than these estimates.

Extended Data Table 2 takes this approach and derives global estimates of H_2 production rates in moles per year using the range of ages for the Proterozoic (rounded up to one billion years (Gyr), and to a maximum of 2.5 Gyr) and for the Archean (2.5 to 3.8 Gyr). The resulting estimates of H_2 production rates from Archean and Proterozoic mafic/ultramafic rocks range from 0.14×10^{11} mol yr^{-1} to 1.6×10^{11} mol yr^{-1} of H_2 for a total global estimate from the Precambrian lithosphere to a depth of 5 km of 0.78×10^{11} mol yr^{-1} to 1.8×10^{11} mol yr^{-1} of H_2 (Extended Data Table 2).

Consideration of the extent of reaction, $\Delta\xi$. Considerations of the likely extent of reaction could provide an even more conservative estimate of H_2 production. The above estimates followed the approach of many of the marine studies, assuming 100% reaction of available FeO (that is, the reaction progress variable $\Delta\xi = 1$; ref. 58). In a second approach, rather than assuming 100% reaction, we assume that $\Delta\xi = 1/2$ in the uppermost kilometre, $\Delta\xi = 1/4$ in the second kilometre, $\Delta\xi = 1/8$ in the third kilometre, and so on, as in ref. 6. Applying this series to the H_2 production rates from 5 km of Precambrian crust derived above (0.78–1.8×10^{11} mol yr^{-1}) reduces estimates to 0.2–0.4×10^{11} mol yr^{-1}. This range of estimated rates 0.2×10^{11} (lower boundary) to 1.8×10^{11} mol yr^{-1} (upper boundary) are the values listed in Table 2.

Erosion and exhumation rates and experimental constraints. It is helpful to explore additional possible approaches for estimating global H_2 production from the Precambrian in order to constrain the estimates discussed above that form the basis for this paper. Two possibilities are to couple the H_2 production based on the reaction-based models either to erosion rates or to the existing (albeit limited) information on experimental rates of H_2 production via hydration reactions[56,59].

As noted, ref. 8's estimate of H_2 production from the marine lithosphere was derived using a different approach from those cited in Table 2 and used 16 H_2 production profiles based on actual H_2 measurements and, for a unit length of ridge axis of a given thickness, calculated a flux by introducing a temporal component using an estimated exhumation rate of 1 cm yr^{-1} (ref. 8). Their reasoning is that the exhumation rate provides the rate of consumption of the crust owing to hydration reactions as exhumation drives propagation of fluid penetration and the reaction front to depth[8]. Applying a similar line of reasoning, the rate of exhumation of the Precambrian lithosphere could be used as an alternative way of incorporating time and deriving rates to compare with those in Extended Data Table 2. Estimates of long-term erosion rates for the Precambrian continents range from ~10 μm yr^{-1} to 2.5 μm yr^{-1} (ref. 60). Taking the total surface area of ultramafic and mafic rock for the Proterozoic and Archean of 3.02×10^{13} m^2 (Extended Data Table 1), even the lower estimate of exhumation rates (2.5 μm yr^{-1}) results in an erosion volume of 7.55×10^7 m^3 yr^{-1}. Given the value of 1.4×10^3 moles H_2 m^{-3} (from equation (4)), this annual erosional volume results in an estimate of H_2 production of 1.06×10^{11} mol yr^{-1}. Hence, this alternative approach yields an estimate in the same range as we provide in Table 2—suggesting that indeed the estimated values calculated in the current study are conservative—given that using higher exhumation rates (up to 10 μm yr^{-1}) would only increase the contribution of H_2 from the Precambrian crust by this approach, to $>4 \times 10^{11}$ mol yr^{-1}.

Using experimentally derived rates of H_2 production is challenging, given both the paucity of such experiments so far, and the inherent difficulty of extrapolating laboratory-derived rates to natural systems. H_2 generation rates via hydration reactions will vary with mineralogy, temperature–pressure–oxygen fugacity, and the degree of mineral alteration[61]. The presence of komatiite (unaltered ultramafic) textures[26] indicates the potential for continuing hydration reactions in Precambrian rocks, although H_2 production rates via hydration reactions in these ancient systems will certainly be slower than in less altered Phanerozoic ophiolites or young ocean floor, owing to the lower temperatures of water–rock reactions in the ancient crust.

Nonetheless, it is useful to explore the implications of H_2 production results via low-temperature water–rock reactions from recent studies. Neubeck *et al.*[59] published CH_4 production rates during weathering of olivine at 30–70 °C of (2.7–7.3) $\times 10^{-11}$ moles per metre squared per second (with an associated H_2 production rate, at an H_2/CH_4 ratio of 4:1, of approximately (10.8–29.2) $\times 10^{-11}$ moles per

metre squared per second). Assuming a surface area per volume of rock of 300 cm^2 per cm^3 (after ref. 16), and extrapolating the rates of ref. 59 to the surface area for Precambrian mafic/ultramafic (Extended Data Table 1; 3.02×10^{13} m^2), the estimated H_2 production over 1 km is of the order of $\sim 1 \times 10^{18}$ mol yr^{-1} of H_2. This is orders of magnitude larger than any of the estimates in the current study (Table 2). This again suggests that the values we derived in this study (Table 2) are conservative, because other published rates of H_2 production from hydration of mafic and ultramafic minerals at $T < 100$ °C report rates[56,62] even greater than those of ref. 59.

30. Wankel, S. D. *et al.* Influence of subsurface biosphere on geochemical fluxes from diffuse hydrothermal fluids. *Nature Geosci.* **4,** 461–468 (2011).
31. Sherwood Lollar, B. *et al.* Evidence for bacterially generated hydrocarbon gas in Canadian Shield and Fennoscandian Shield rocks. *Geochim. Cosmochim. Acta* **57,** 5073–5085 (1993a).
32. Sherwood Lollar, B. *et al.* Abiogenic methanogenesis in crystalline rocks. *Geochim. Cosmochim. Acta* **57,** 5087–5097 (1993b).
33. Ward, J. A. *et al.* Microbial hydrocarbon gases in the Witwatersrand Basin, South Africa: implications for the deep biosphere. *Geochim. Cosmochim. Acta* **68,** 3239–3250 (2004).
34. Sherwood Lollar, B. *et al.* Unravelling abiogenic and biogenic sources of methane in the Earth's deep subsurface. *Chem. Geol.* **226,** 328–339 (2006).
35. Vovk, I. F. in *Saline Water and Gases in Crystalline Rocks* Special Paper 33 (eds Fritz, P. & Frape, S. K.) 197–210 (Geological Society of Canada, 1987).
36. Potter, J., Rankin, A. H. & Treloar, P. J. Abiogenic Fischer-Tropsch synthesis of hydrocarbons in alkaline igneous rocks: fluid inclusion, textural and isotopic evidence from the Lovozero complex, N.W. Russia. *Lithos* **75,** 311–330 (2004).
37. Pedersen, K. *Microbial Processes in Radioactive Waste Disposal.* Report TR-00-04 (Swedish Nuclear Fuel and Waste Management Company (SKB), 2000).
38. Morrill, P. L. *et al.* Geochemistry and geobiology of a present-day serpentinization site in California: the Cedars. *Geochim. Cosmochim. Acta* **109,** 222–240 (2013).
39. Fritz, P., Clark, I. D., Fontes, J.-C., Whiticar, M. J. & Faber, E. in *Water-Rock Interaction* Vol. 1 *Low Temperature Environments* (ed Kharaka, Y. & Maest, A. S.) 793–796 (1992).
40. Neal, C. & Stanger, G. Hydrogen generation from mantle source rocks in Oman. *Earth Planet. Sci. Lett.* **66,** 315–320 (1983).
41. Abrajano, T. A. *et al.* Geochemistry of reduced gas related to serpentinization of the Zambales ophiolite, Philippines. *Appl. Geochem.* **5,** 625–630 (1990).
42. Coveney, R. M., Jr, Goebel, E. D., Zeller, E. J., Dreschhoff, G. A. M. & Angine, E. E. Serpentinization and the origin of hydrogen gas in Kansas. *Am. Assoc. Petrol. Geol. Bull.* **71,** 39–48 (1987).
43. Newell, K. D. *et al.* H_2-rich and hydrocarbon gas recovered in a deep Precambrian well in Northeastern Kansas. *Nat. Resour. Res.* **16,** 277–292 (2007).
44. Salters, V. J. M. & Stracke, A. Composition of the depleted mantle. *Geochem. Geophys. Geosyst.* **5,** 1–27 (2004).
45. Jaehne, B., Heinz, G. & Dietrich, W. Measurement of the diffusion coefficients of sparingly soluble gases in water. *J. Geophys. Res.* **92,** 10767–10776 (1987).
46. Lippmann, J. *et al.* Dating ultra-deep mine waters with noble gases and ^{36}Cl, Witwatersrand Basin, South Africa. *Geochim. Cosmochim. Acta* **67,** 4597–4619 (2003).
47. Aquilina, L., de Dreuzy, J. R., Bour, O. & Davy, P. Porosity and fluid velocities in the upper continental crust (2 to 4 km) inferred from injection tests at the Soultz-sous-Forets geothermal site. *Geochim. Cosmochim. Acta* **68,** 2405–2415 (2004).
48. Bucher, K. & Stober, I. Fluids in the upper continental crust. *Geofluids* **10,** 241–253 (2010).
49. Stober, I. Permeabilities and chemical properties of water in crystalline rocks of the Black Forest, Germany. *Aquat. Geochem.* **3,** 43–60 (1997).
50. Stober, I. & Bucher, K. Hydraulic properties of the crystalline basement. *Hydrogeol. J.* **15,** 213–224 (2007).
51. Silver, B. J. *et al.* The origin of NO_3^- and N_2 in deep subsurface fracture water of South Africa. *Chem. Geol.* **294–295,** 51–62 (2012).
52. Savary, V. & Pagel, M. The effects of water radiolysis on local redox conditions in the Oklo, Gabon natural fission reactors 10 and 16. *Geochim. Cosmochim. Acta* **61,** 4479–4494 (1997).
53. Lowenstern, J. B., Evans, W. C., Bergfeld, D. & Hunt, A. G. Prodigious degassing of a billion years of accumulated radiogenic helium at Yellowstone. *Nature* **506,** 355–358 (2014).
54. Charlou, J. L., Donval, J. P., Fouquet, Y., Jean-Baptiste, P. & Holm, N. Geochemistry of high H_2 and CH_4 vent fluids issuing from ultramafic rocks at the Rainbow hydrothermal field (36°14''N, MAR). *Chem. Geol.* **191,** 345–359 (2002).
55. Andreani, M., Daniel, I. & Pollet-Villard, M. Aluminum speeds up the hydrothermal alteration of olivine. *Am. Mineral.* **98,** 1738–1744 (2013).
56. Mayhew, L. E., Ellison, E. T., McCollom, T. M., Trainor, T. P. & Templeton, A. S. Hydrogen generation from low-temperature water-rock reactions. *Nature Geosci.* **6,** 478–484 (2013).
57. Kelemen, P. B. & Hirth, G. Reaction-driven cracking during retrograde metamorphism: olivine hydration and carbonation. *Earth Planet. Sci. Lett.* **345–348,** 81–89 (2012).
58. Helgeson, H. C. in *Geochemistry of Hydrothermal Ore* (ed. Barnes, H. L.) 568–610 (Wiley, 1979).
59. Neubeck, A., Duc, N. T., Bastviken, D., Crill, P. & Holm, N. G. Formation of H_2 and CH_4 by weathering of olivine at temperatures between 30 and 70°C. *Geochem. Trans.* **12,** http://dx.doi.org/10.1186/1467-4866-12-6 (2011).
60. Flowers, R. M., Bowring, S. A. & Reiners, P. W. Low long-term erosion rates and extreme continental stability documented by ancient (U-Th)/He dates. *Geology* **34,** 925–928 (2006).
61. McCollom, T. M. & Bach, W. Thermodynamic constraints on hydrogen generation during serpentinization of ultramafic rocks. *Geochim. Cosmochim. Acta* **73,** 856–875 (2009).
62. Stevens, T. O. & McKinley, J. P. Abiotic controls on H_2 production from basalt-water reactions and implications for aquifer biogeochemistry. *Environ. Sci. Technol.* **34,** 826–831 (2000).

Extended Data Table 1 | Volumes of mafic/ultramafic rock with H_2 production potential and H_2 production to depths of 1 km and 5 km

Continental Lithosphere	% †	Surface Area (10^7 km^2)	% Mafic & Ultramafic ‡	Volume Mafic & Ultramafic to 1 km (x 10^{16} m^3)	Moles H_2 to 1 km (x 10^{19}) §	Moles H_2 to 5 km (x 10^{19}) §
Proterozoic	86	9.12	25	2.28	3.19	16.0
Archean	14	1.48	50	0.74	1.04	5.2
TOTAL Precambrian *	100	10.60	-	3.02	4.23	21.2

(See Methods for detailed calculations and discussion.)
* Based on total surface area for Precambrian continental lithosphere of 1.06×10^8 km^2 (ref. 12).
† Based on Proterozoic and Archean surface areas, accounting for 86% and 14%, respectively, of the total Precambrian continental surface area (refs 12 and 27).
‡ Mafic and ultramafic from ref. 26.
§ Based on 1.4×10^3 moles H_2 per cubic metre of mafic and ultramafic rock from equation (4) (Methods) and based on $\Delta\xi = 1$ (100% reaction efficiency).

Extended Data Table 2 | Estimated H_2 production rates from Precambrian mafic/ultramafic rock for a 5 km volume

Continental Lithosphere	Moles H_2 to 5 km ($\times 10^{19}$) *	Minimum Age ($\times 10^9$ yr)	Moles H_2 per year ($\times 10^{11}$)	Maximum Age ($\times 10^9$ yr)	Moles H_2 per year ($\times 10^{11}$)
Proterozoic †	16.0	1.0	1.6	2.5	0.64
Archean	5.2	2.5	0.2	3.8	0.14
TOTAL Precambrian	21.2	-	1.8	-	0.78

(See Methods for detailed calculations and discussion.)
* From Extended Data Table 1.
† Minimum age for Proterozoic rounded up to 1.0 Gyr. Using values of <1 Gyr would only increase the estimates of H_2 production rates in this table. Throughout this study, we attempted to provide lower boundaries on H_2 production (conservative estimates). Actual production is thus likely to be higher.